European Journal of Mineralogy

Composition and crystal structure of grundmannite, CuBiSe2, the Se-analogue of emplectite, a new mineral from the El Dragón mine, Potosí, Bolivia

--Manuscript Draft--

Manuscript Number:	
Article Type:	Research paper
Full Title:	Composition and crystal structure of grundmannite, CuBiSe2, the Se-analogue of emplectite, a new mineral from the El Dragón mine, Potosí, Bolivia
Short Title:	Composition and crystal structure of grundmannite, CuBiSe2,
Corresponding Author:	Hans-Jürgen Förster Deutsches GeoForschungsZentrum GFZ Potsdam, GERMANY
Corresponding Author E-Mail:	forhj@gfz-potsdam.de
Order of Authors:	Hans-Jürgen Förster
	Luca Bindi
	Chris J. Stanley
Abstract:	Grundmannite, ideally CuBiSe2, is a new mineral species from the El Dragón mine, Department of Potosí, Bolivia. It is either filling small shrinkage cracks or interstices in brecciated kruta'ite−penroseite solid solutions or forms independent grains in the matrix. Grain size of the anhedral to subhedral crystals is usually in the range 50−150 μm, but may approach 250 μm. Grundmannite is usually intergrown with watkinsonite and clausthalite; other minerals occasionally being in intimate grain-boundary contact comprise quartz, dolomite, native gold, eskebornite, umangite, klockmannite, Co-rich penroseite, and three unnamed phases of the Cu−Bi−Hg−Pb−Se system, among which is an as-yet uncharacterizedspecies with the ideal composition Cu4Pb2HgBi4Se11. Eldragónite and petrovicite rarely precipitated in the neighborhood of CuBiSe2. Grundmannite is non-fluorescent, black and opaque with a metallic luster and black streak. It is brittle, with an irregular fracture and no obvious cleavage and parting. The VHN20 values range from 45 to 61 (mean 53) kg mm−2, which equals to a Mohs hardness of 2 to 2½. In plane-polarized incident light, grundmannite is weakly bireflectant and weakly pleochroic, from cream to light grey, and shows no internal reflections. Between crossed polars, grundmannite is distinctly anisotropic, with light brown to brown rotation tints. The reflectances in air for the COM standard wavelengths are: 41.0−43.4 (470 nm), 41.8−45.1 (546 nm), 42.1−45.7 (589 nm), and 42.5−46.2 (650 nm). Electron-microprobe analyses yielded a mean composition Cu 14.88, Pb 1.23, Hg 007, Ni 0.05, Bi 44.90, Se 38.92, total 100.05 wt.%. The mean empirical formula, normalized to 4 atoms per formula unit (apfu), is Cu0.99(Bi0.91Pb0.02)∑0.93Se2.08 (n = 19). The ideal formula is CuBiSe2, which requires Cu 14.76, Bi 48.55 and Se 36.69 wt%. Grundmannite is orthorhombic, space group Pnma, with a 6.6362(5), b 4.2581(3), c 15.3691(9) Å, V 434.29(5) Å3, and Z = 4. Density calculated on the basis of the mean chemical composition and unit-cell parameters derived from the single-crystal X-ray study is 6.582 g cm−3. The five strongest X-ray powder-diffraction lines [d in Å (I/I0) (hkl)] are: 3.4901 (50) (111), 3.3180 (70) (200), 3.2746 (100) (013), 2.4923 (45) (015), and 2.3307 (50) (213). The crystal structure of grundmannite is topologically identical to that of emplectite, CuBiS2, with the two independent sulfur positions occupied by Se, thus being the Se-analogue of emplectite. In the structure, Bi forms BiSe3 trigonal pyramids (with two additional longer distances) and Cu nearly regular CuSe4 tetrahedra. Grundmannite is a primary mineral, deposited from an oxidizing low-T hydrothermal fluid at the waning stage of selenide-mineral formation at El Dragón, at a fSe2/fS2 ratio greater than unity and in the presence of hematite, conditions typically prevailing during the formation of telethermal vein-type selenide deposits. The mineral was named after Günter Grundmann, in recognition of his pioneering work on the El Dragón mine.
Keywords:	grundmannite; new mineral species; chemical composition, crystal structure; bismuth; copper; selenium; Cu−Pb−Hg−Bi−Se system; Cu4Pb2HgBi4Se11; El

	Dragón
Manuscript Region of Origin:	GERMANY
Requested Editor:	Reto Gieré
Suggested Reviewers:	Cristian Biagoni University of Pisa biagioni@dst.unipi.it
	Anthony R. Kampf Natural History Museum of Los Angeles County akampf@nhm.org
	Frantisek Laufek Czech Geological Survey frantisek.laufek@geology.cz
	Mark D. Welch Natural History Museum, London m.welch@nhm.ac.uc
Opposed Reviewers:	
Additional Information:	
Question	**Response**
Author Comments:	

Composition and crystal structure of grundmannite, $CuBiSe_2$, the Se-analogue of emplectite, a new mineral from the El Dragón mine, Potosí, Bolivia

HANS-JÜRGEN FÖRSTER[1,*], LUCA BINDI[2] and CHRIS J. STANLEY[3]

[1] Helmholtz Centre Potsdam German Research Centre for Geosciences GFZ,
D-14473 Potsdam, Germany
*Corresponding author, e-mail: hans-juergen.foerster@gfz-potsdam.de

[2] Dipartimento di Scienze della Terra, Università degli Studi di Firenze,Via G. La Pira 4,
I-50121 Firenze, Italy

[3] Department of Earth Sciences, Natural History Museum, Cromwell Road,
London SW7 5BD, United Kingdom

Abstract: Grundmannite, ideally $CuBiSe_2$, is a new mineral species from the El Dragón mine, Department of Potosí, Bolivia. It is either filling small shrinkage cracks or interstices in brecciated kruta'ite–penroseite solid solutions or forms independent grains in the matrix. Grain size of the anhedral to subhedral crystals is usually in the range 50–150 µm, but may approach 250 µm. Grundmannite is usually intergrown with watkinsonite and clausthalite; other minerals occasionally being in intimate grain-boundary contact comprise quartz, dolomite, native gold, eskebornite, umangite, klockmannite, Co-rich penroseite, and three unnamed phases of the Cu–Bi–Hg–Pb–Se system, among which is an as-yet uncharacterizedspecies with the ideal composition $Cu_4Pb_2HgBi_4Se_{11}$. Eldragónite and petrovicite rarely precipitated in the neighborhood of $CuBiSe_2$. Grundmannite is non-fluorescent, black and opaque with a metallic luster and black streak. It is brittle, with an irregular fracture and no obvious cleavage and parting. The VHN_{20} values range from 45 to 61 (mean 53) kg mm^{-2}, which equals to a Mohs hardness of 2 to 2½. In plane-polarized incident light, grundmannite is weakly bireflectant and weakly pleochroic, from cream to light grey, and shows no internal reflections. Between crossed polars, grundmannite is distinctly anisotropic, with light brown to brown rotation tints. The reflectances in air for the COM standard wavelengths are: 41.0–43.4 (470 nm), 41.8–45.1 (546 nm), 42.1–45.7 (589 nm), and 42.5–46.2 (650 nm). Electron-microprobe

analyses yielded a mean composition Cu 14.88, Pb 1.23, Hg 007, Ni 0.05, Bi 44.90, Se 38.92, total 100.05 wt.%. The mean empirical formula, normalized to 4 atoms per formula unit (*apfu*), is $Cu_{0.99}(Bi_{0.91}Pb_{0.02})_{\sum 0.93}Se_{2.08}$ (n = 19). The ideal formula is $CuBiSe_2$, which requires Cu 14.76, Bi 48.55 and Se 36.69 wt%. Grundmannite is orthorhombic, space group *Pnma*, with *a* 6.6362(5), *b* 4.2581(3), *c* 15.3691(9) Å, *V* 434.29(5) Å^3, and *Z* = 4. Density calculated on the basis of the mean chemical composition and unit-cell parameters derived from the single-crystal X-ray study is 6.582 g cm^{-3}. The five strongest X-ray powder-diffraction lines [*d* in Å (*I*/*I*$_0$) (*hkl*)] are: 3.4901 (50) (111), 3.3180 (70) (200), 3.2746 (100) (013), 2.4923 (45) (015), and 2.3307 (50) (213). The crystal structure of grundmannite is topologically identical to that of emplectite, $CuBiS_2$, with the two independent sulfur positions occupied by Se, thus being the Se-analogue of emplectite. In the structure, Bi forms $BiSe_3$ trigonal pyramids (with two additional longer distances) and Cu nearly regular $CuSe_4$ tetrahedra. Grundmannite is a primary mineral, deposited from an oxidizing low-*T* hydrothermal fluid at the waning stage of selenide-mineral formation at El Dragón, at a fSe_2/fS_2 ratio greater than unity and in the presence of hematite, conditions typically prevailing during the formation of telethermal vein-type selenide deposits. The mineral was named after Günter Grundmann, in recognition of his pioneering work on the El Dragón mine.

Key-words: grundmannite; new mineral species; chemical composition, crystal structure; selenide; bismuth; copper; selenium; Cu−Pb−Hg−Bi−Se system; $Cu_4Pb_2HgBi_4Se_{11}$; El Dragón; Bolivia

1. Introduction

In the Andes of South America, the province of La Rioja in Argentina hosts one of the most important selenium mineralizations on Earth (*e.g.*, Paar *et al.*, 2012, and references therein). The state of Bolivia is well known for two minor, but scientifically interesting selenide occurrences: Pacajake, district of Hiaco de Charcas, and El Dragón, Province of Quijarro, both in the Department of Potosí. The geology and ore mineralization of the El Dragón mine was first explored in detail by Grundmann *et al.* (1990); it subsequently received further attention as the type locality of eldragonite, $Cu_6BiSe_4(Se_2)$, and two unnamed species of the Cu−Hg−Pb−Bi−Se system (Paar *et al.*, 2012), and the description of the new secondary Pb−Bi−Cu selenite favreauite, $PbBiCu_6O_4(SeO_3)_4(OH) \cdot H_2O$ (Mills *et al.*, 2014).

A renewed comprehensive study of a large number of ore-bearing samples from El Dragón collected during two field campaigns in 1987 and 1988 by a research team from the Technische Universität München, Germany, revealed the presence of another Cu−Bi sulfosalt with the composition $CuBiSe_2$, constituting the Se-analogue of emplectite, $CuBiS_2$. The description of this new selenium mineral, grundmannite, forms the subject of this paper. The

natural existence of a mineral of the composition $CuBiSe_2$ was first implied from quantitative microprobe data of unknown species present in the complex selenium mineralization at Altenberg a.d.Rax (Steiermark, Austria), but neither compositional nor structural data were provided (Niedermayr *et al*., 1997).

The new species grundmannite and its name have been approved by the Commission on New Minerals, Nomenclature and Classification (CNMNC) of the IMA, proposal 2015−038. The holotype specimen, which is the section from which the grain used for crystal-structure determination was obtained, is deposited in the collections of the Natural History Museum, London, catalogue number BM 2015, 33. Cotype material, consisting of a grundmannite-bearing section, is housed within the Mineralogical States Collection Munich (Mineralogische Staatssammlung München, Museum "Reich der Kristalle"), under the inventory number MSM 73584. The mineral name is in honour of Günter Grundmann (b. 1947), in recognition of his pioneering work on the El Dragon mine (*e.g.*, Grundmann *et al*., 1990).

2. Location and Geology

The El Dragón selenide occurrence is situated in southwestern Bolivia, in the Cordillera Oriental, some 30 km southwest of Cerro Rico de Potosi. The abandoned El Dragon mine (entrance and dump) is located 19° 49' 23.90" S (latitude), 65° 55' 00.60" (longitude), at an altitude of 4160 m above sea level. It is about 4 km east of the Porco Caldera hosting one of the largest Ag−Zn−Pb−Sn deposits in Bolivia (Cunningham *et al*., 1993). The Porco mining district has a long history of production, beginning in pre-Columbian times when Indians mined it for silver. The very small longitudinal extension (maximum 15-m-long gallery) of the El Dragón selenium ore vein and its low silver content (0.06 wt.% Ag) have probably discouraged the occurrence to be further exploited.

The adit of the El Dragón mine is on the orographic left side of the Rio Jaya Mayu, cutting through a series of thinly-stratified, pyrite-rich black shales and reddish-grey, hematite-bearing siltstones of probably Devonian age, dipping 40° to the north. The almost vertical ore vein is located in the center of a 1.5-m-wide shear zone (average trend 135 degrees) with shifts of a few cm. In 1988, the selenium mineralization consisted of a single vein, ranging mostly from 0.5 to 2 cm in thickness, with sporadic bulges of up to 6 cm.

3. Occurrence and associated minerals

The El Dragón mineralization is composed of a complex assemblage of partially rare primary and secondary minerals, among which Se-bearing phases are most prominent. The full list of minerals recorded from El Dragón is given on mindat.org at http://www.mindat.org/loc-353.html. Grundmann *et al.* (1990) and Paar *et al.* (2012) provided detailed descriptions of the entire mineralization. Here we focus on grundmannite and associated primary minerals of the system Cu−Bi−Hg−Pb−Se. A comprehensive discussion of the origin of the El Dragón mineralization will form the subject of a forthcoming paper.

During this study, a total of 125 polished thick sections of average size 2 x 2 cm and average weight 8 g and several polished vein sections of up to 4 cm in thickness with adhesive wall rock fragments were examined macroscopically and microscopically. Grundmannite was detected in only 10% of the inspected thick sections. Other associated Cu−Bi-bearing selenides are comparatively more frequent. Thus, watkinsonite was present in almost all inspected samples, eldragónite in about two thirds of the sections.

4. Appearance and physical properties

The appearance and paragenetic associations of grundmannite and other Bi-selenides are visualized in Figures 1 and 2, resp. constituting collections of optical microscopy photographs and back-scattered electron (BSE) images.

Grundmannite commonly forms sub- to anhedral grains up to 150 µm in size typically intergrown with clausthalite (PbSe; Figs. 1a-c, 2a-b) and associated with kruta'ite−penroseite solid solutions (Cu_2Se−Ni_2Se; Figs. 1a-d). These solid solutions usually form systematically zoned grains, with Cu-rich compositions resembling kruta'ite in the cores evolving towards more Ni−(Co)-rich compositions in the direction to the grain margins, with penroseite s.s. at the outermost rims. Grundmannite also appear as aggregates of irregularly shaped grains of several hundreds of µm across associated with the same species as above (Fig. 1b). Grundmannite occasionally shows parallel intergrowths of grains, implied from serrated prismatic grain surfaces. Intergrowths with watkinsonite are frequent (Figs. 1a-d). Other minerals occasionally being in intimate grain-boundary contact with grundmannite comprise quartz, dolomite, native gold (Fig. 1c), eskebornite ($CuFeSe_2$), umangite (Cu_3Se_2),

klockmannite (CuSe), discrete grains of Co-rich penroseite, unnamed phases "A" and "B" of Paar *et al.* (2012), and a newly discovered species of the Cu−Bi−Hg−Pb−Se system termed phase "C" (*cf.* section Chemical composition). Eldragónite (Fig. 1b) and petrovicite rarely precipitated in the surroundings of $CuBiSe_2$. Grundmannite partially replaces umangite, klockmannite, eskebornite and native gold and itself became partially decomposed by late fracture-filling chalcopyrite (Fig. 1d). Secondary minerals in the neighbourhood of grundmannite encompass chalcomeneite, 'clinochalcomeneite', favreauite, molybdomeneite, ahlfeldite, 'kersteneite', olsacherite, schmiederite, goethite, and late klockmannite.

About half of the identified grundmannite grains is cementing (usually together with clausthalite and watkinsonite) shrinkage cracks and or filling interstices in breacciatedkruta'ite−penroseite solid solutions, the other half formed as independent grains in the matrix. Grundmannite was never observed as inclusions in kruta'ite−penroseite.

Grundmannite is non-fluorescent, black and opaque with a metallic luster and black streak. It is brittle, with an irregular fracture and no obvious cleavage and parting. The mean Vickers hardness number (VHN) for a 20 g load is 53 kg mm^{-2} (range 45−61). This number equates to a Mohs hardness of 2 to 2½. Density could not be measured because of the small grain size. Density calculated on the basis of the mean chemical composition and unit-cell parameters derived from the single-crystal X-ray study is 6.582 g cm^{-3}.

5. Optical properties

In plane-polarized incident light, grundmannite is cream to light grey in colour, weakly bireflectant and weakly pleochroic from cream to light grey. The mineral does not show any internal reflections. Between crossed polars, grundmannite is distinctly anisotropic, with light brown to brown rotation tints.

Quantitative reflectance data for grundmannite were obtained in air relative to a Zeiss WTiC standard using a J & M TIDAS diode array spectrometer attached to a Zeiss Axiotron microscope. Measurements were made on unoriented grains at extinction positions leading to designation of R_1 (minimum) and R_2 (maximum). The results are listed in Table 1 (together with the calculated color values) and illustrated graphically in Figure 3. From 400 to 700 nm, the reflectance values of R_1 are smoothly ascending continuously toward the longer wavelengths. The values of R_2 display the same systematics, but the increase is more rapid.

6. Chemical Composition

Ore minerals from El Dragón were routinely checked for concentrations of Cu, Ag, Pb, Hg, Fe, Co, Ni, As, Sb, Bi, S and Se. Quantitative chemical analyses of grundmannite and the remaining selenides were conducted in WDS mode, using a JEOL thermal field-emission-type electron probe X-ray microanalyzer (FE-EPMA) JXA-8500F (HYPERPROBE) at the Deutsches GeoForschungsZentrum GFZ, Potsdam, Germany. The probe was operated at 20 kV, 20 nA; the beam size was 1−2 µm. The counting time on peak was 20s, with half that time on background on both sites of the peak. Special care was taken to avoid any elemental interferences on peak and backgrounds, or empirically correct them. The following standards, emission lines and analyzing crystals (in parentheses) were used: Cu – native Cu metal, *K*α (LIF); Ag – natural Ag_2Se, *L*α (PETJ); Pb – natural PbSe, *M*α (PETH); Hg – natural HgS, *L*α (LIF); Fe – natural FeS_2, *K*α (LIF); Co – natural $(Co,Ni)As_3$, *K*α (LIF); Ni – natural $(Fe,Ni)_9S_8$, *K*α (LIF); As - natural $(Co,Ni)As_3$, *L*α (TAP); Sb – natural Sb_2S_3, *L*α (PETJ), Bi – synthetic Bi_2Se_3, *M*α (PETH); S – natural ZnS, K*α* *K*α (PETJ); Se – natural Ag_2Se, *K*α (LIF). The CITZAF routine in the JEOL software, which is based on the ϕ(ρZ) method (Armstrong, 1995), was used for data processing.

6.1 Grundmannite

Grundmannite from El Dragón displays an only a weak variation in composition in all samples studied in this paper (Table 2). In addition to the major cations Cu, Bi and Se, the only other element continuously present is Pb, with concentrations between 1.0 and 1.3 wt%. Subordinate amounts of Hg (< 0.3 wt.%) and Ni (< 0.2 wt%) were detected occasionally. Substitution of divalent Pb for trivalent Bi explains the observed slight deviation from ideal stoichiometry. The mean empirical formula, normalized to 4 atoms per formula unit (*apfu*), is $Cu_{0.99}(Bi_{0.91}Pb_{0.02})_{\sum 0.93}Se_{2.08}$ (n = 19). The ideal formula is $CuBiSe_2$, thus being the Se-analogue of emplectite, $CuBiS_2$, as confirmed by structural data.

6.2 Associated Cu−Bi−(Pb)−(Hg)−Se minerals

The mean compositions (together with the number of analyzed spots) and 1δ standard deviations and the respective formula proportions for petrovicite, watkinsonite, eldragónite, and unnamed phases “A”, “B” and “C” are listed in Table 3. Except for the newly established phase “C”, the compositional data reported here are slightly different from those measured by Paar *et al.* (2012), but generally confirm the observations and conclusions made by these authors.

Petrovicite, ideally $Cu_3HgPbBiSe_5$, has the composition $(Cu_{2.97}Ag_{0.04})_{\sum 3.01}Hg_{0.99}Pb_{0.99}Bi_{1.03}Se_{4.98}$, based on 15 *apfu* . Silver is omnipresent as a minor element (0.2−0.8 wt%). As already recognized by Paar *et al.* (2012), the composition of watkinsonite, ideally $Cu_2PbBi_4Se_8$, is characterized by the substitution of variable, but uncommonly large concentrations of Ag for Cu. The concentrations of Ag range between 1.3 and 5.2 wt%, which is equivalent to 9−44 mol% $Ag_2PbBi_4Se_8$ and suggest the possible existence of an Ag-analogue of watkinsonite in nature. The other omnipresent cation in the watkinsonite structure is Hg, with concentrations in the range 0.3−1.3 wt%. Nickel occurs sporadically, with concentrations maximizing to 0.3 wt%. The mean formula of watkinsonite yields $(Cu_{1.53}Ag_{0.44}Ni_{0.02})_{\sum 1.99}(Pb_{1.08}Hg_{0.07})_{\sum 1.15}Bi_{3.88}Se_{7.98}$, normalized to 15 atoms per formula unit. With respect to the elevated abundances of Ag und Hg, watkinsonite from El Dragón closely resembles watkinsonite from Schlema-Alberoda in the Erzgebirge of Germany, which has the mean formula $(Cu_{1.47}Ag_{0.49}Cd_{0.02}Ni_{0.01})_{\sum 1.99}(Pb_{1.01}Hg_{0.01})_{\sum 1.02}Bi_{3.98}(Se_{7.98}S_{0.05})_{\sum 8.03}$ (Förster *et al.*, 2003).

Our analytical data for phases "A" and "B" confirmed the formula projections made by Paar *et al.* (2012), but yielded analytical totals relatively closer to 100 wt% (cf. Table 3). Phase "A", with the ideal formula $Cu_5Pb_2HgBi_3Se_{10}$, has the mean formula $(Cu_{4.90}Ag_{0.22})_{\sum 5.12}Pb_{1.90}Hg_{0.89}Ni_{0.06}Co_{0.01}Bi_{3.09}Se_{9.92}$, normalized to 22 *apfu*. Between 0.4 and 1.3 wt.% Ag was substituted for Cu. Nickel is continuously present, with concentrations between <0.1 and 0.6 wt.%. Phase "B" exhibits the ideal formula $Cu_2PbHgBi_2Se_6$ and has the mean composition $(Cu_{2.05}Ag_{0.10})_{\sum 2.15}Pb_{0.91}Hg_{0.80}Ni_{0.04}Co_{0.01}Bi_{2.08}Se_{6.01}$ (on the basis of 12 *apfu*). As phase "A", this species contains minor concentrations of Ag (0.4−1.8 wt.%) and Ni (<0.5 wt%). The analytical data acquired for phase "C" would meet the ideal formula $Cu_4Pb_2HgBi_4Se_{11}$; its mean formula amounts to $(Cu_{3.45}Ag_{0.50})_{\sum 4.95}Pb_{2.05}Hg_{0.91}Ni_{0.05}Co_{0.01}Fe_{0.01}Bi_{4.01}Se_{11.00}$ (on the basis of 22 *apfu*). Noteworthy, there are elevated concentrations of Ag (1.8−2.3 wt.), most probably sitting on the Cu-position, and trace amounts of Ni (<0.3 wt.%).

The composition of phase "C" requires additional remarks. Thus, this species may be chemically more variable than reflected by its mean composition provided in Table 3 and a single spot analyses presented in Table 1 (ana.#1). Spot analyses performed in relatively brighter domains in intergrowths of phases "A" and "B" also revealed compositions that are distinct by larger concentrations of Fe (up to 1.4 wt.%) or Ni (up to 0.4 wt.%) (Table 4, ana.# 2−4). If these data did not suffer from analytical shortcomings owing to the small domain size and the intimate intergrowth with other selenides, they would also fit the ideal composition $Cu_4Pb_2HgBi_4Se_{11}$ at the precondition that Fe and Ni (and Co) are part of the Cu-position (Fe

and Ni are strongly negatively correlated with Cu). If these compositions refer to phase "C", one quarter of the Cu-position could be accommodated by Ag (Table 4, ana.# 4). Crystal-structure data are required to resolve this problem, for the acquisition of which suitable material was not available.

7. Crystal structure

7.1 X-ray powder-diffraction data

The observed powder diffraction pattern (Table 5) of the same grundmannite fragment used for the single-crystal study (see below) was collected with a CCD-equipped diffractometer Xcalibur PX Ultra using Cu*K*α radiation (50 kV and 40 mA – 5 hs as exposition time). Crystal-to-detector distance was 7 cm. Data were processed using the *CrysAlis* software package version 1.171.31.2 (Oxford diffraction 2006) running on the Xcalibur PX control PC. The unit-cell parameters obtained from powder data are: a = 6.6331(2), b = 4.2551(2), c = 15.3782(6) Å, V = 434.04(2) Å^3, in excellent agreement with those obtained from single-crystal data.

7.2 X-ray single-crystal data

Three grundmannite fragments were mounted on a 0.005 mm diameter carbon fiber (which was, in turn, attached to a glass rod) and checked on a CCD-equipped Oxford Diffraction Xcalibur 3 single-crystal diffractometer, operating with Mo*K*α radiation (λ = 0.71073 Å). One of them (size: 75 × 80 × 95 μm) showed an excellent diffraction quality and the full data collection was done (Table 6). Intensity integration and standard Lorentz-polarization corrections were performed with the *CrysAlis* RED (Oxford Diffraction, 2006) software package. The program ABSPACK of the *CrysAlis* RED package (Oxford Diffraction, 2006) was used for the absorption correction. Reflection conditions were consistent with the space group *Pnma*, the space group observed for emplectite (Kyono & Kimata, 2005) that can be considered the S-analogue of grundmannite. The full-matrix least-squares program SHELXL-97 (Sheldrick, 2008), working on F^2, was used for the refinement of the structure, which was carried out starting from the atomic coordinates reported for emplectite (Kyono & Kimata, 2005). Site-scattering values were refined using scattering curves for neutral species (Ibers & Hamilton 1974) as follows: Cu vs. □ and Bi vs. □ for the cation sites, and S vs. □ for the anion sites. All the sites were found fully occupied, and the occupancy factors were then fixed to 1.00. The electron density refined at the metal sites is in excellent agreement with the

electron-microprobe data (Table 2). Successive cycles were run introducing anisotropic temperature factors for all the atoms leading to R_1 = 0.0247 for 611 observed reflections [$F_o > 4\sigma(F_o)$] and R_1 = 0.0250 for all 818 independent reflections. Fractional atomic coordinates and isotropic atomic displacement parameters are reported in Table 7 whereas the bond distances are given in Table 8. Structure factors and CIF are freely available online as Supplementary Material linked to this article on the GSW website of the journal, http://eurjmin.geoscienceworld.org/.

8. Results and Discussion

8.1 Crystal-chemical remarks

The crystal structure of grundmannite (Fig. 4) is topologically identical to that of emplectite, $CuBiS_2$ (Kyono & Kimata, 2005), with the two independent sulfur positions occupied by Se. In the structure, Bi forms $BiSe_3$ trigonal pyramids (with two additional longer distances) and Cu nearly regular $CuSe_4$ tetrahedra (Table 8). The entry of Se in the emplectite structure induces a strong enlargement of the unit-cell as well as in the coordination environment of Bi and Cu. The orthorhombic modification of $CuBiSe_2$ has been not synthesized yet but calculations, using the first-principles DFT method, have shown that such a compound is thermodynamically stable (Kumar & Persson, 2014) and that the chalcostibite−emplectite (*Pnma*) structure is retained. The calculated unit-cell parameters for the $CuBiSe_2$ compound are a = 6.58, b = 4.11, c = 15.05 Å, in close agreement with those measured in this work for grundmannite. The standard thermodynamic properties of $CuBiSe_2$ were calculated by Babanly *et al.* (2009). The $Cu(Sb,Bi)(S,Se)_2$ compounds are orthorhombic-type semiconductors (Kumar & Persson, 2014).

Emplectite and grundmannite resulted to be isostructural. Although this could be easily guessed given the similarity of S and Se, there are many phases in the Cu−Ag−S−Se group of minerals that are not isostructural. Amongst this group, acanthite (Ag_2S, S.G. $P2_1/n$, Frueh, 1958) and naumannite (Ag_2Se, S.G. $P2_12_12_1$, Wiegers, 1971) and stromeyerite (CuAgS, S.G. $Cmc2_1$, Baker *et al.*, 1991) and eucairite (CuAgSe, S.G. *Pmmn*, Frueh *et al.*, 1957) are not isostructural, whereas metacinnabar (HgS, S.G. *F*-43*m*, Aurivillius, 1964) and tiemannite (HgSe, S.G. *F*-43*m*, Earley, 1950) and thalcusite ($Cu_2FeTl_2S_4$, S.G. *I*4/*mmm*, Makovicky *et al.*, 1980) and bukovite ($Cu_2FeTl_2Se_4$, S.G. *I*4/*mmm*, Makovicky *et al.*, 1980) are isostructural. As to the IMA sulfosalt systematics (Moëlo *et al.*, 2008), grundmannite is a

294 binary sulfosalt and the third member of the emplectite isotypic series, after emplectite and
295 chalcostibite ($CuSbS_2$).

296 **8.2 Origin of grundmannite**

297 A re-study of a large collection of ore and country-rock samples from El Dragón provided
298 strong evidence that the available genetic concepts on the origin of this unique mineralization
299 (Grundmann *et al.*, 1990; Paar *et al*., 2012) require substantial revision and will be presented
300 elsewhere. The most likely source of Se and accompanying elements (Cu, Co, Ni, Pb, Bi,
301 Ag,…) is of the Kupferschiefer-type: reduced black shale rich in framboidal pyrite, copper
302 sulfides, and organic material. The Se-mineralization was deposited in a fault zone at the
303 contact of that shale with a hematite-rich, oxidized siltstone. Our genetic model involves the
304 transport and deposition of Se and accompanying elements from the same low-*T*
305 hydrothermal fluid (likely a heated descending meteoric water) during one single event.
306 Kruta'ite−penroseite solid solutions were among the first selenides that crystallized from that
307 solution, thus enriching it in elements incompatible with its structure, mainly Pb, Bi, and Hg.
308 Grundmannite postdates the kruta'ite−penroseite solid solutions and appears to also
309 crystallize later than the bulk of accompanying Cu−Bi−(Pb)−(Hg)−Se minerals. Together
310 with later generations of watkinsonite and clauthalite, it constitutes the youngest primary Se-
311 mineral forming the El Dragón deposit, precipitated probably in the stability fields of
312 umangite and klockmannite. Thermodynamic properties and calculated phase equilibria of
313 selenides (Simon & Essene, 1996) permit to broadly constrain the fugacities of Se_2 and S_2
314 during grundmannite crystallization. Thus, the absence of berzelianite and bellidoite suggests
315 that the selenium fugacity was in a range from below the kruta'ite−klockmannite univariant
316 reaction to above the umangite−berzelianite univariant reaction. For a temperature of 100 °C
317 typical for most telethermal vein-type deposits, this range corresponds to $\log f Se_2$ between
318 −10.5 to −14.5 (Simon & Essene, 1997). The presence of hematite/goethite and the absence of
319 chalcopyrite, pyrite and bornite imply sulfur fugacities that maximized to $\log f S_2$ of roughly
320 −17, but most likely were much lower considering the remarkable sulfur paucity of all Se-
321 minerals. Thus, the crystallization environment of grundmannite includes a fSe_2/fS_2 ratio
322 greater than unity and the presence of hematite, conditions typically prevailing during the
323 formation of telethermal vein-type selenide mineralization (Simon & Essene, 1997).

Acknowledgements: First of all, our sincere thanks go to Günter Grundmann, who provided the samples from El Dragón studied in the paper, called the first author's attention to the presence of unidentified minerals in these specimens, and actively supported our work with a pre-inspection of the polished sections by optical microscopy. He, together with G. Lehrberger, F. Grüner and A. Zwicker (Technsche Universität München), collected the samples, from which the holotype material was obtained. The study of the El Dragón and Pacajake selenide occurrences was part of the 'International Scientific Cooperation' European Community−Andean Pact Countries, 4 Earth Sciences, Joint Research Project No. 9 'Rare metals in Bolivian ores', managed by G. Morteani (Report: EUR 14495 EN, 1993, ISBN 92-826-4547-9). Dieter Rhede (formerly Deutsches GeoForschungsZentrum GFZ, Potsdam, Germany) is acknowledged for his valuable support with the electron-microprobe analyses and the effort he spent on improving the analytical routines for the quantitative analysis of complex selenium minerals. One of us (CJS) acknowledges Natural Environment Research Council grant NE/M010848/1 Tellurium and Selenium Cycling and Supply.

References

Armstrong, J.T. (1995): CITZAF: a package of correction programs for the quantitative electron microbeam X-ray-analysis of thick polished materials, thin films, and particles. *Microbeam Anal*., **4**, 177–200.Aurivillius, K. (1964): An x-ray and neutron diffraction study of metacinnabarite. *Acta Chem. Scand.*, **18**, 1552–1553.

Babanly, N.B., Yusibov, Yu.A., Aliev, Z.S., Babanly, M.B. (2010): Phase equilibria in the Cu−Bi−Se system and thermodynamic properties of copper selenobismuthates. *Russ. J. Inorg. Chem*., 55, 1471−1481.

Baker, C.L., Lincoln, F.J., Johnson, A.W.S. (1991): A low-temperature structural phase transformation in CuAgS. *Acta Crystallogr.*, **B47**, 891–899.

Criddle, A.D. & Stanley, C.J. (1993): Quantitative Data File for Ore Minerals, 3rd Edition. Chapman and Hall/ Natural History Museum London.

Cunningham, C.A., Aparicio, H.N., Murillo, F.S., Jiménez, N.Ch., Lizeca, J.-L.B., McKee, E.H., Ericksen, G.E., Tavera, F.V. (1993): The relationship between the Porco, Bolivia, Ag−Zn−Pb−Sn deposit, and the Porco caldera. *US Geol. Surv., Open-File Report 94-238*.

Earley, J.W. (1950): Description and synthesis of the selenide minerals. *Am. Mineral.*, **35**, 337–364.

Förster, H.-J., Cooper, M.A., Roberts, A.C., Stanley, C.J., Criddle, A.J., Hawthorne, F.C., Laflamme, J.H.G., Tischendorf, G. (2003): Schlemaite, $(Cu□)_6(Pb,Bi)Se_4$ a new mineral species from Niederschlema−Alberoda, Erzgebirge, Germany: description and crystal structure. *Can. Mineral.* **41**, 1433–1444.

Frueh, A.J.,Jr. (1958): The crystallography of silver sulfide, Ag_2S. *Z. Krist.*, **110**, 136–144.

Frueh, A.J.,Jr., Czamanske, G.K., Knight, Ch. (1957): The crystallography of eucairite, CuAgSe. *Z. Krist.*, **108**, 389–396.

Grundmann, G., Lehrberger, G., Schnorrer-Köhler, G. (1990): The El Dragón mine, Potosí, Bolivia. *Mineral. Rec*., **21**, 133−146.Ibers, J.A. & Hamilton, W.C. Eds. (1974): *International Tables for X-ray Crystallography*, vol. IV, 366p. Kynock, Dordrecht, The Netherlands.

Johan, Z., Picot, P., Ruhlmann, F.(1987): The ore mineralogy of the Otish Mountains uranium deposit, Quebec: skippenite, Bi_2Se_2Te, and watkinsonite, $Cu_2PbBi_4(Se,S)_8$, two new mineral species. *Canad. Mineral.*, **25**, 625−638.

Kumar, M. & Persson, C. (2014): $Cu(Sb,Bi)(S,Se)_2$ as indium-free absorber material with high optical efficiency. *Energy Procedia*, **44**, 176–183.

Kyono, K. & Kimata, M. (2005): Crystal structures of chalcostibite ($CuSbS_2$) and emplectite ($CuBiS_2$): Structural relationship of stereochemical activity between chalcostibite and emplectite. *Am. Mineral.*, **90**, 162–165.

Makovicky, E., Johan, Z., Karup-Møller, S. (1980): New data on bukovite, thalcusite, chalcothallite and rohaite. *N. Jb. Miner. Abh.*, **138**, 122–146.

Mills, S. J.,Kampf, A.R., Christy, A.G., Housley, R. M., Thorne, B., Chen, Yu-Sheng, Steele, I. M. (2014): Favreauite, a new selenite mineral from the El Dragón mine, Bolivia. *Eur. J. Mineral.*, **26**, 771−781.

Moëlo, Y., Makovicky, E., Mozgova, N.N., Jambor, J.L., Cook, N., Pring, A., Paar, W., Nickel, E.H., Graeser, S., Karup-Møller, S., Balic-Žunic, T., Mumme, W.G., Vurro, F., Topa, D., Bindi, L., Bente, K., Shimuzu, M. (2008): Sulfosalt systematics: Report oft the sulfosalt-subcommittee of the IMA Commission on New Minerals. *Eur. J. Mineral.*, **20**, 7−46.

Niedermayr, G., Bernhard, F., Bojar, H.-P., Brandstätter, F., Ettinger, K., Moser, B., Paar, W.H., Postl, W., Taucher, J., Walter, F. (1997): Neue Mineralfunde aus Österreich XLVI. *Carintia II*, **187**, 169−214.

Oxford Diffraction (2006): *CrysAlis* RED (Version 1.171.31.2) and ABSPACK in *CrysAlis* RED. Oxford Diffraction Ltd, Abingdon, Oxfordshire, England.

Paar, W.H., Cooper, M.A., Moëlo, Y., Stanley, C.J., Putz, H., Topa, D., Roberts, A.C., Stirling, J., Raith, J.G., Rowe, R. (2012): Eldragónite, $Cu_6BiSe_4(Se)_2$, a new mineral species from the El Dragón mine, Potosí, Bolivia, and its crystal structure. *Can. Mineral.*, **50**, 281−294.

Picot, P. & Johan, Z. (1982): Atlas of Ore Minerals. Elsevier/BRGM.

Sheldrick, G.M. (2008): A short history of SHELX. *Acta Crystallogr.*, **A64**, 112–122.

Simon, G. & Essene, E.J. (1996): Phase relations among selenides, sulphides, tellurides, and oxides: I. Thermodynamic properties and calculated equilibria. *Econ. Geol.*, **91**, 1183−1208.

Simon, G. & Essene, E.J. (1997): Phase relations among selenides, sulphides, tellurides, and oxides: II: Applications to selenide-bearing ore deposits. *Econ. Geol.*, **92**, 468−484.

Wiegers, G.A. (1971): The crystal structure of the low-temperature form of silver selenide. *Am. Mineral.*, **56**, 1882−1888.

Table titles

Table 1. Reflectance data and color values for grundmannite.

Table 2. Composition of grundmannite (wt.%) from El Dragón.

Table 3. Mean composition (wt.%) and formula proportions of Cu−Bi selenides associated with grundmannite.

Table 4. Results of spot analyses of phase "C".

Table 5. Calculated and observed X-ray powder diffraction data for grundmannite.

Table 6. Data and experimental details for the selected grundmannite crystal.

Table 7. Atom coordinates and equivalent isotropic displacement parameters ($Å^2$) for grundmannite.

Table 8. Selected bond distances (Å) and angles (°) for grundmannite.

Figure captions

Figure 1. Reflected light images of (a) the grain of grundmannite, from which the structural and reflectance data were obtained (horizontal field (h.f.) ~ 250 μm); (b) grundmannite, watkinsonite, eldragonite, klockmannite, and clausthalite as fracture filling in intensely zoned kruta'ite−penroseite solid solutions (h.f. ~ 500μm); (c) grundmannite+clausthalite+watkinsonite replaced by native Au (h.f. ~ 500 μm); (d) grundmannite+watkinsonite+ kruta'ite−penroseite replaced by chalcopyrite along fractures (h.f. ~ 200 μm); (e) intimate intergrown of eldragónite, phase "A" and various other selenides (h.f. ~ 200 μm); (f) petrovicite associated with a plethora of other selenium-bearing minerals filling a fracture in krutàite−penroseite (h.f. ~ 500μm). Abbreviations of mineral names: kps.s. = kruta'ite−penroseite solid solutions, gru = grundmannite, wat = watkinsonite, cl = clausthalite, pen = penroseite, kl = klockmannite, cha = chalcopyrite, eld = eldragónite, pet = petrovicite,, "A" phase "A" of Paar *et al.* (2012).

Figure 2. Microprobe-generated back-scattered electron images of (a) anhedral to subhedral grains of grundmannite (medium bright) and clauthalite (bright) enclosing kruta'ite−penroseite crystals; (b) irregularly shaped grundmannite intergrown with clausthalite; c) intergrowth of phases "A"and "B" with watkinsonite and clausthalite; (d) phases "A" ,"B" and "C" (for chemical composition see Table 3) in grain contact; (e) mineral aggregate composed of phases "A" (medium bright), "B" (least bright)

and “C” (most bright; for compositional data see Table 4, ana.#4); (f) clausthalite intergrown with petrovicite and inhomogeneous acicular crystals mainly composed of phase “B” filling a fracture in kruta’ite−penroseite solid solutions, in contrast to eldragónite occurring inside. See Fig. 1 for abbreviations of mineral names.

Figure 3. Reflectance spectra of grundmannite, its S-analogue emplectite, and other Cu−Bi selenides in air. Data sources: eldragónite – Paar *et al.* (2012); schlemaite – Förster *et al.* (2003); emplectite – Criddle & Stanley (1993); watkinsonite – Johan *et al.* (1987); petrovicite – Picot & Johan (1982).

Figure 4. The crystal structure of grundmannite projected down [010]. The horizontal direction is the *a*-axis. Cu atoms are depicted as blue tetrahedral, Bi and Se are given as violet and green spheres, respectively. Dashed lines indicate long Bi−Se distances. The unit cell is outlined.

Figure

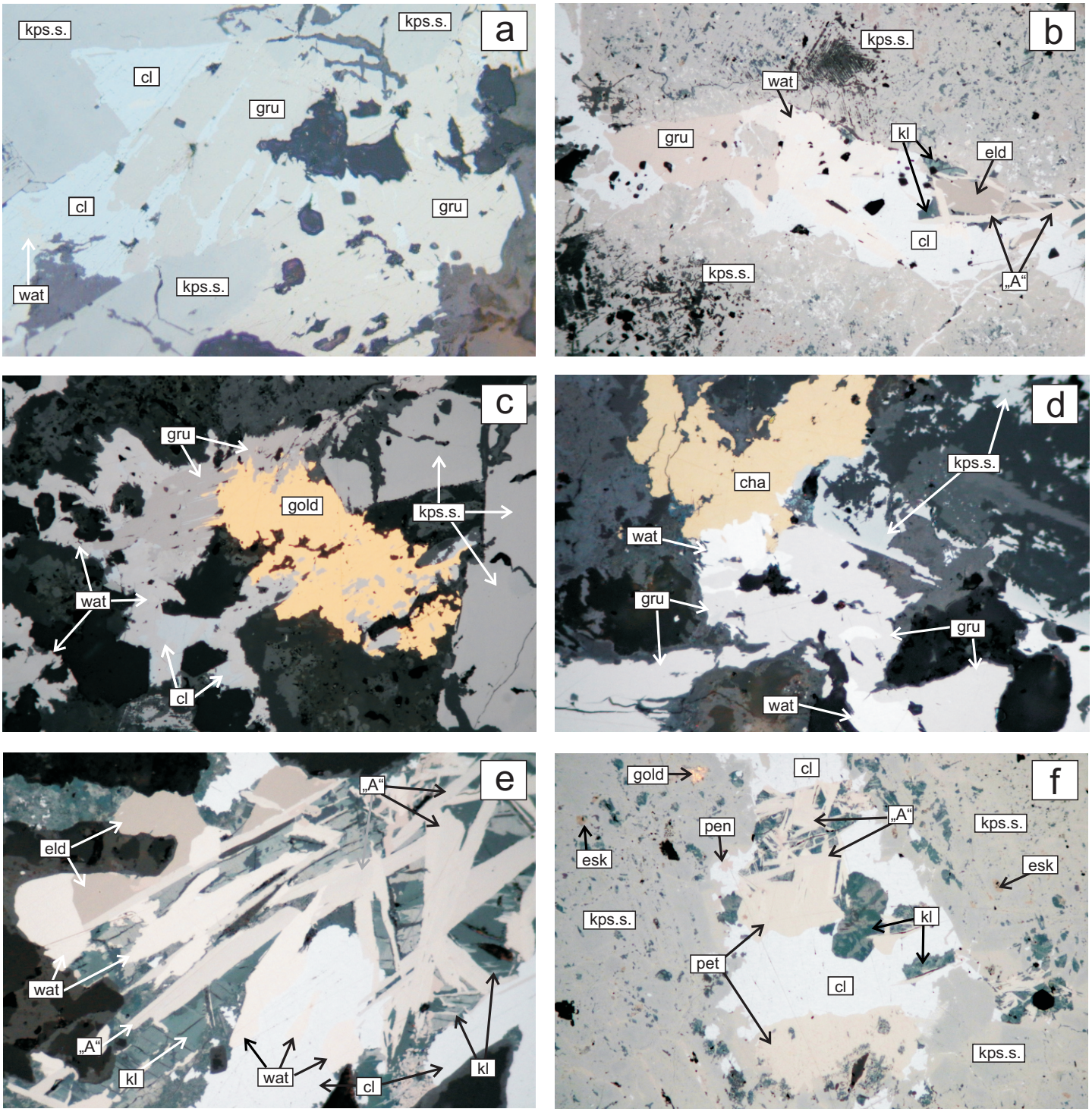
a
kps.s.
kps.s.
cl
gru
cl
gru
wat
kps.s.
b
kps.s.
wat
gru
kl
eld
cl
kps.s.
„A“
c
gru
gold
kps.s.
wat
cl
d
cha
kps.s.
wat
gru
gru
wat
e
„A“
eld
wat
„A“
kl
wat
cl
kl
f
gold
cl
„A“
pen
kps.s.
esk
esk
kps.s.
kl
pet
cl
kps.s.

Figure

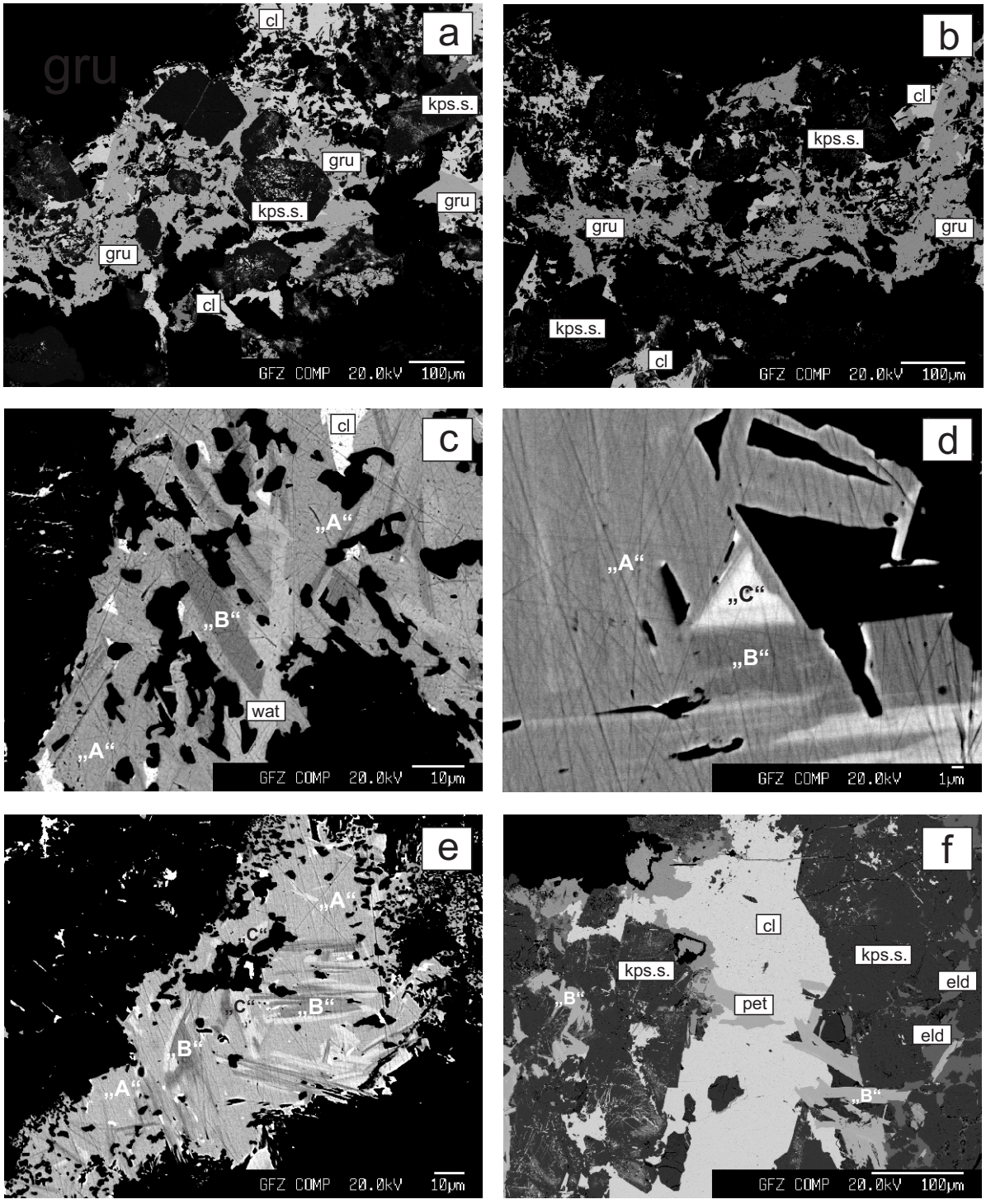
a
cl
gru
kps.s.
gru
gru
kps.s.
gru
cl
GFZ COMP 20.0kV 100µm
b
cl
kps.s.
gru
gru
kps.s.
cl
GFZ COMP 20.0kV 100µm
c
cl
„A“
„B“
wat
„A“
GFZ COMP 20.0kV 10µm
d
„A“
„C“
„B“
GFZ COMP 20.0kV 1µm
e
„A“
„C“
„C“
„B“
„B“
„A“
GFZ COMP 20.0kV 10µm
f
cl
kps.s.
kps.s.
eld
„B“
pet
eld
„B“
GFZ COMP 20.0kV 100µm

Figure

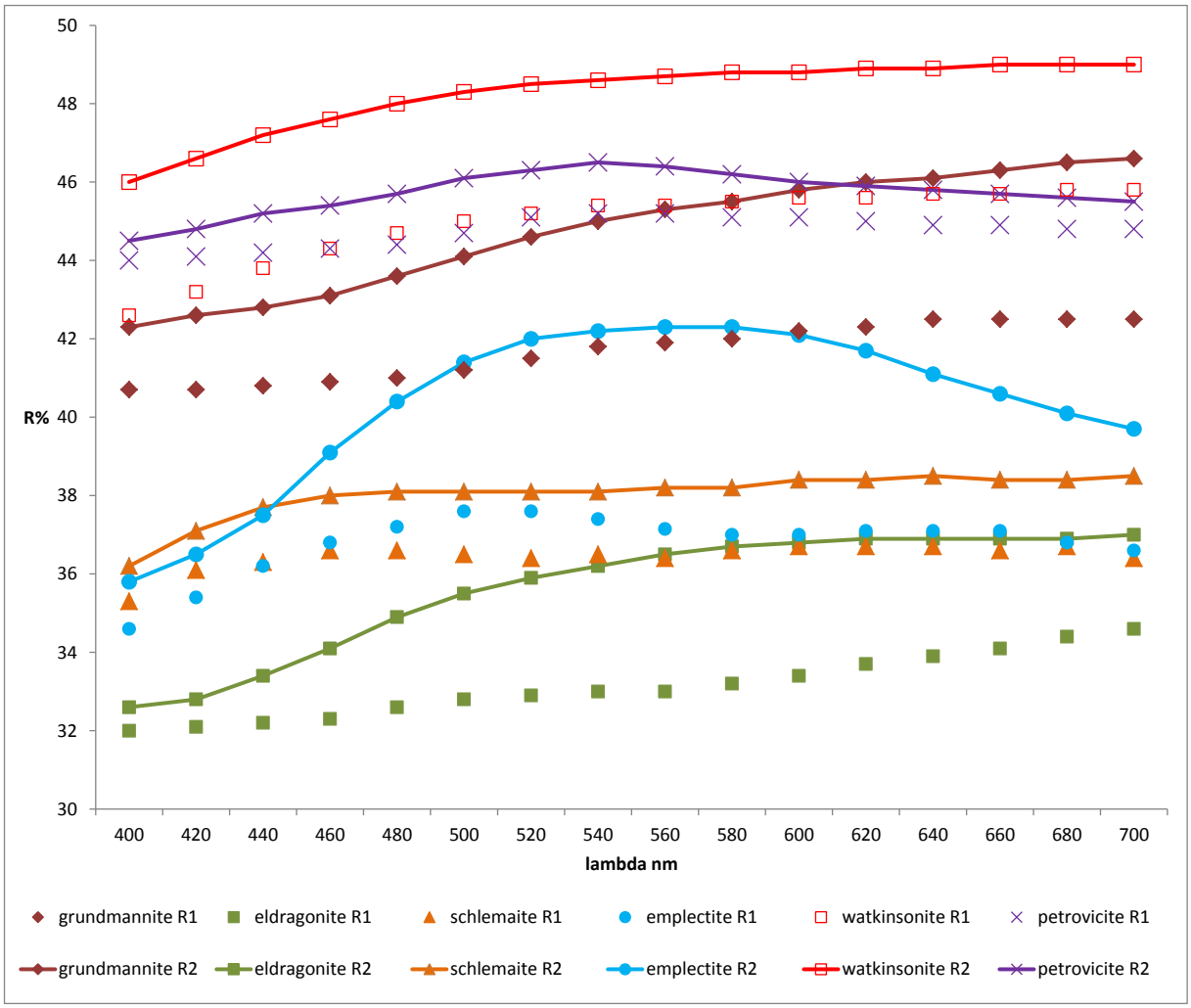
50
48
46
44
42
40
38
36
34
32
30
R%
400
420
440
460
480
500
520
540
560
580
600
620
640
660
680
700
lambda nm
grundmannite R1
eldragonite R1
schlemaite R1
emplectite R1
watkinsonite R1
petrovicite R1
grundmannite R2
eldragonite R2
schlemaite R2
emplectite R2
watkinsonite R2
petrovicite R2

Figure

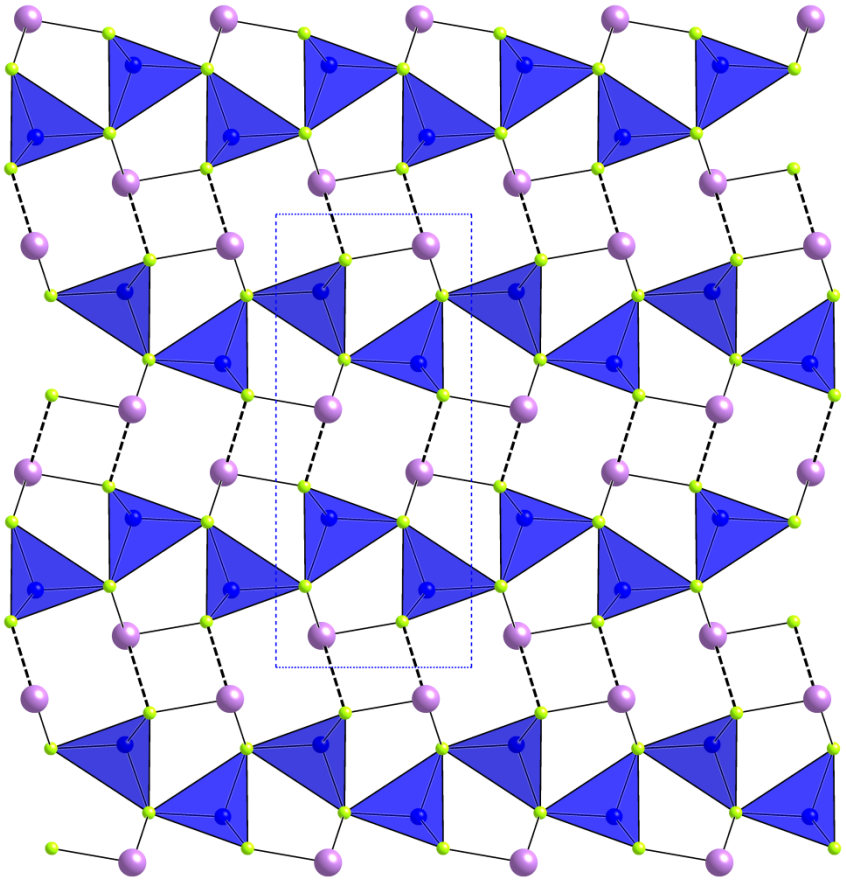

Table

Table 1. Reflectance data and color values for grundmannite.

λ (nm)	R_1 (%)	R_2 (%)	λ (nm)	R_1 (%)	R_2 (%)
400	40.7	42.3	640	42.5	46.1
420	40.7	42.6	660	42.5	46.3
440	40.8	42.8	680	42.5	46.5
460	40.9	43.1	700	42.5	46.6
480	41.0	43.6			
500	41.2	44.1	Commission on Ore Mineralogy		
520	41.5	44.6	wavelengths		
540	41.8	45.0			
560	41.9	45.3	470	41.0	43.4
580	42.0	45.5	546	41.8	45.1
600	42.2	45.8	589	42.1	45.7
620	42.3	46.0	650	42.5	46.2

Color values

	C illuminant		A illuminant	
	R_1	R_2	R_1	R_2
x	0.313	0.316	0.450	0.452
y	0.319	0.322	0.408	0.409
Y (%)	41.8	45.1	42.0	45.4
l_d	577	576	586	586
P_e (%)	1.7	3.1	2.5	4.4

Table

Table 2. Composition of grundmannite (wt.%) from El Dragón.

	Cu	Hg	Pb	Ni	Bi	Se	Total
mean	14.88	0.07	1.23	0.05	44.9	38.92	100.05
1δ	0.11	0.10	0.10	0.06	0.24	0.24	0.32
min	14.69	0.00	0.99	0.00	44.62	38.44	99.38
max	15.05	0.30	1.38	0.22	45.53	39.33	100.81

Notes: 1δ = 1δ standard deviation.

Table

Table 3. Mean composition (wt.%) and formula proportions of Cu−Bi selenides associated with grundmannite.

	petrovicite		watkinsonite		eldragonite		phase "A"		phase "B"		phase "c"	
n	8		39		11		24		28		4	
	aver.	1δ	aver.	1δ	aver.	1δ	aver.	1δ	aver.	1δ	aver.	1δ
Cu	15.51	0.35	5.33	0.83	34.18	0.18	13.34	0.28	9.31	0.43	8.53	0.23
Ag	0.45	0.24	2.62	1.20	0.10	0.05	1.02	0.28	0.73	0.25	2.12	0.20
Hg	16.51	0.19	0.83	0.40	0.01	0.02	7.67	0.22	11.43	0.30	7.08	0.27
Pb	17.12	0.13	12.23	0.43	0.00	0.00	16.87	0.13	13.55	0.24	16.54	0.21
Fe	0.00	0.00	0.01	0.03	1.47	0.23	0.00	0.00	0.00	0.00	0.02	0.03
Co	0.00	0.00	0.00	0.01	0.02	0.04	0.03	0.04	0.03	0.03	0.02	0.02
Ni	0.01	0.03	0.05	0.17	0.21	0.19	0.15	0.15	0.17	0.14	0.12	0.11
Bi	17.80	0.07	44.52	0.68	19.83	0.13	27.65	0.19	31.17	0.26	32.59	0.18
S	0.00	0.00	0.00	0.00	0.00	0.00	0.00	0.00	0.00	0.00	0.00	0.00
Se	32.55	0.11	34.53	0.54	44.33	0.16	33.52	0.20	34.00	0.32	33.75	0.07
total	99.93	0.50	100.12	0.87	100.16	0.49	100.24	0.30	100.40	0.46	100.76	0.09
apfu	11		15		13		21		12		22	
Cu	2.97	0.03	1.53	0.24	5.71	0.05	4.90	0.09	2.05	0.09	3.45	0.09
Ag	0.04	0.01	0.44	0.21	0.01	0.01	0.22	0.06	0.10	0.03	0.50	0.05
Hg	0.99	0.01	0.07	0.02			0.89	0.03	0.80	0.02	0.91	0.04
Pb	0.99	0.01	1.08	0.03			1.90	0.02	0.91	0.02	2.05	0.02
Fe					0.28	0.04					0.01	0.01
Co						0.01	0.01	0.02	0.01	0.01	0.01	0.01
Ni			0.02	0.02	0.04	0.03	0.06	0.06	0.04	0.03	0.05	0.05
Bi	1.03	0.00	3.88	0.05	1.01	0.01	3.09	0.03	2.08	0.03	4.01	0.03
Se	4.98	0.01	7.98	0.04	5.96	0.03	9.92	0.04	6.01	0.05	11.00	0.03

Notes: n = number of spot analyses averaged, 1δ = 1δ standard deviation.

Table

Table 4. Results of spot analyses of phase "C".

ana.#	1	2	3	4
Cu	8.53	6.51	6.77	6.66
Ag	2.19	3.32	2.29	4.11
Hg	7.32	7.01	7.20	7.22
Pb	16.41	16.39	16.15	16.37
Fe	0.00	0.38	1.43	0.00
Co	0.00	0.09	0.06	0.13
Ni	0.11	0.39	0.25	0.40
Bi	32.43	32.37	33.05	32.55
Se	33.78	33.31	33.30	33.00
Total	100.76	99.77	100.50	100.45
Cu (*apfu*)	3.45	2.69	2.75	2.74
Ag	0.52	0.81	0.55	1.00
Hg	0.94	0.92	0.93	0.94
Pb	2.04	2.07	2.01	2.07
Fe	0.00	0.18	0.66	0.00
Co	0.00	0.04	0.02	0.06
Ni	0.05	0.17	0.11	0.18
Bi	3.99	4.06	4.08	4.08
Se	11.01	11.06	10.89	10.94

Notes: cations normalized to 4 *apfu*.

Table 5. Calculated and observed X-ray powder diffraction data for grundmannite.

hkl	d_{calc} (Å)	I_{calc}	d_{obs} (Å)	I_{obs}
002	7.6845	17.11	-	-
102	5.0225	23.10	5.01	15
004	3.8423	18.82	3.83	15
111	3.4901	49.45	3.49	50
104	3.3251	30.54	3.32	70
200	3.3180	57.24		
013	3.2746	100.00	3.27	100
112	3.2479	13.01	3.24	25
201	3.2433	15.30		
202	3.0462	6.29	3.05	5
113	2.9365	7.56	2.940	10
203	2.7849	7.16	2.785	10
015	2.4923	40.52	2.490	45
212	2.4775	8.55	2.478	10
106	2.3897	12.40	2.390	15
213	2.3307	44.97	2.329	50
020	2.1290	33.31	2.128	35
215	1.9927	30.98	1.995	35
017	1.9514	11.64	1.952	10
311	1.9471	31.69	1.946	30
008	1.9211	10.28	1.922	10
304	1.9170	21.83	1.918	20
312	1.9019	5.71	-	-
117	1.8722	11.66	1.874	10
024	1.8622	5.18	-	-
216	1.8306	9.98	1.832	10
124	1.7930	10.56	1.796	10
220	1.7919	20.07	1.790	20
221	1.7798	5.66	-	-
314	1.7480	5.29	-	-
208	1.6626	9.74	1.664	10
126	1.5896	7.13	1.590	5
119	1.5416	11.17	1.542	10
317	1.4634	6.66	1.465	5
028	1.4263	7.51	1.425	25
324	1.4246	15.96		
033	1.3678	7.20	1.368	5
228	1.3103	8.15	1.310	10
233	1.2646	5.82	1.262	15
511	1.2628	9.87		
504	1.2545	7.16	1.253	5
235	1.2012	5.06	-	-
331	1.1910	5.45	-	-
524	1.0808	7.67	-	-

Notes: calculated diffraction pattern obtained with the atom coordinates reported in Table 7 (only reflections with $I_{rel} \geq 5$ are listed).

Table

Table 6. Data and experimental details for the selected grundmannite crystal.

Crystal data	
Formula	$CuBiSe_2$
Crystal size (mm)	0.075 × 0.080 × 0.095
Form	block
Colour	black
Crystal system	orthorhombic
Space group	*Pnma*
a (Å)	6.6362(5)
b (Å)	4.2581(3)
c (Å)	15.3691(9)
V (Å^3)	434.29(5)
Z	4
Data collection	
Instrument	Oxford Diffraction Xcalibur 3
Radiation type	Mo*K*α (λ = 0.71073 Å)
Temperature (K)	293(2)
Detector to sample distance (cm)	5
Number of frames	677
Measuring time (s)	60
Maximum covered 2θ (°)	70.00
Absorption correction	multi-scan (*ABSPACK*; Oxford Diffraction 2006)
Collected reflections	7621
Unique reflections	818
Reflections with $F_o > 4\,\sigma\,(F_o)$	611
R_{int}	0.0257
R_σ	0.0546
Range of *h, k, l*	$-10 \le h \le 10, -6 \le k \le 6, -24 \le l \le 24$
Refinement	
Refinement	Full-matrix least squares on F^2
Final R_1 [$F_o > 4\,\sigma\,(F_o)$]	0.0247
Final R_1 (all data)	0.0250
Number of least squares parameters	25
Goodness of Fit	1.175
$\Delta\rho_{max}$ (e Å^{-3})	1.20
$\Delta\rho_{min}$ (e Å^{-3})	−1.33

Table

Table 7. Atom coordinates and equivalent isotropic displacement parameters (Å^2) for grundmannite.

atom	*x*/*a*	*y*/*b*	*z*/*c*	U_{iso}*/U_{eq}
Cu	0.22875(10)	¼	0.82957(5)	0.02068(13)
Bi	0.23364(3)	¼	0.069531(15)	0.02469(8)
Se1	0.64523(9)	¼	0.10055(4)	0.03118(12)
Se2	0.85020(10)	¼	0.82089(5)	0.03310(13)

Table

Table 8. Selected bond distances (Å) and angles (°) for grundmannite.

Ca1	
Ca1	
Ca1	
Ca1	
In1	
In1	
In	
S1	
S1	
S1	
S1	
S1	
S1	
S1	
S1	
S1	
S1	

Symmetry codes: (i) *x*−1/2, *y*, −*z*+3/2; (ii) *x*−1, *y*, *z*; (iii) −*x*+1, −*y*+1, −*z*+1; (iv) −*x*+1, −*y*, −*z*+1; (v) *x*+1/2, *y*, −*z*+3/2; (vi) *x*+1, *y*, *z*.

This piece of the submission is being sent via mail.